

See discussions, stats, and author profiles for this publication at: <https://www.researchgate.net/publication/47334960>

# Electronic Transitions of Protonated Benzene and Fulvene, and of C<sub>6</sub>H<sub>7</sub> Isomers in Neon Matrices

ARTICLE in JOURNAL OF THE AMERICAN CHEMICAL SOCIETY · OCTOBER 2010

Impact Factor: 12.11 · DOI: 10.1021/ja106470x · Source: PubMed

---

CITATIONS

21

---

READS

36

## 4 AUTHORS, INCLUDING:



Jan Fulara

University of Basel

78 PUBLICATIONS 1,659 CITATIONS

SEE PROFILE



John P. Maier

University of Basel

517 PUBLICATIONS 8,399 CITATIONS

SEE PROFILE

Electronic Transitions of Protonated Benzene and Fulvene,  
and of C<sub>6</sub>H<sub>7</sub> Isomers in Neon MatricesIryna Garkusha, Jan Fulara,<sup>†</sup> Adam Nagy, and John P. Maier\*Department of Chemistry, University of Basel, Klingelbergstrasse 80,  
CH-4056 Basel, Switzerland

Received July 21, 2010; E-mail: j.p.maier@unibas.ch

**Abstract:** Electronic transitions of protonated benzene ( $\tilde{A}^1B_2 \leftarrow \tilde{X}^1A_1$ , origin at 325 nm) and  $\alpha$ -protonated fulvene ( $\tilde{A}^1A' \leftarrow \tilde{X}^1A'$ , at 335 nm) trapped in 6 K neon matrices have been detected. The cations were produced from several different precursors, mass-selected, and co-deposited with neon. After neutralization of the cations, the electronic transitions of cyclohexadienyl (onsets at 549 and 310 nm) and  $\alpha$ -hydrogenated fulvene (532 and 326 nm) radicals were identified. Upon excitation of cyclohexadienyl to the  $\tilde{B}^2B_1$  state, photoisomerization to an open-chain structure and  $\alpha$ -hydrogenated fulvene was observed.

## 1. Introduction

The benzenium ion is recognized as the most stable isomer of C<sub>6</sub>H<sub>7</sub><sup>+</sup> and represents a fundamental class of organic ions. It was found to be an intermediate ( $\sigma$ -complex) in electrophilic substitution on aromatic rings, an important reaction of aromatic hydrocarbons.<sup>1</sup> C<sub>6</sub>H<sub>7</sub><sup>+</sup> cations have also been detected by mass spectrometry in the ionosphere of Titan.<sup>2</sup> In this context, the reactivity of ionized polycyclic aromatic hydrocarbons (PAHs) with simple atomic and molecular species was investigated.<sup>3,4</sup> It was found, for example, that benzene cations reacted readily with atomic hydrogen but not with H<sub>2</sub>. Protonated PAHs are relatively stable toward addition of further atomic hydrogen due to their closed-shell electronic structures.

C<sub>6</sub>H<sub>7</sub><sup>+</sup> ions have been studied as complexes with noble gas atoms by infrared photodissociation (IRPD) spectroscopy.<sup>5,6</sup> These investigations have provided frequencies of several fundamentals of C<sub>6</sub>H<sub>7</sub><sup>+</sup>: rare gas dimers in the range 750–3400 cm<sup>-1</sup>. A group of bands near 2800 cm<sup>-1</sup> was attributed to the aliphatic C–H stretches of the methylene group of the benzenium ion.<sup>5</sup> Due to the weak interaction between C<sub>6</sub>H<sub>7</sub><sup>+</sup> and noble gas atoms, the obtained IR frequencies should not differ much from those of the isolated ions.

Multiphoton IRPD spectra of C<sub>6</sub>H<sub>7</sub><sup>+</sup> cations,<sup>7</sup> which undergo H<sub>2</sub> loss, differ from the spectra mentioned above. The observed bands are broadened, red-shifted and vary in intensity from single-photon dissociation data, which could be explained by the nature of the multiphoton fragmentation process. These IR

studies in combination with *ab initio* calculations have confirmed that benzenium ion in its <sup>1</sup>A<sub>1</sub> ground state (C<sub>2v</sub> symmetry) is the favored form of C<sub>6</sub>H<sub>7</sub><sup>+</sup>. The structure is planar, with the exception of the CH<sub>2</sub> hydrogens, which lie in a plane perpendicular to that of the benzene ring.

Electronic spectroscopy on protonated benzene is limited to absorption in superacidic solutions<sup>8</sup> and low-resolution UV photodissociation investigations.<sup>9</sup> The gas-phase spectrum revealed two broad, structureless transitions around 330 and 245 nm, which differ significantly from the solution spectra. Interpretations based on early quantum chemical calculations were given.<sup>9</sup> Recent *ab initio* calculations<sup>10</sup> on excited electronic states provide an assignment for the UV spectrum of this cation.

Not much is known about other isomers of C<sub>6</sub>H<sub>7</sub><sup>+</sup>. A number of investigations, mainly mass spectrometric, have been reported on the structures of C<sub>6</sub>H<sub>7</sub><sup>+</sup> cations. Besides protonated benzene, they all predict at least three additional geometries of interest. The next two most stable forms of this ion,  $\alpha$ - and  $\beta$ -protonated fulvenes, were found mainly on the basis of proton affinities. The former lies 0.4 and the latter 1.3 eV above the benzenium ion according to calculations.<sup>11,12</sup> The most stable open-chain isomer is located even higher (by 1.7 eV).<sup>12</sup>

Formation of protonated fulvene, in addition to benzenium ion, likely occurs upon dissociative ionization of a number of C<sub>6</sub>H<sub>8</sub> isomers<sup>13,14</sup> or by ion–molecule reactions involving allene, propyne,<sup>14,15</sup> butadiene,<sup>16</sup> allyl bromide,<sup>17</sup> vinyl chloride,<sup>18</sup> and

<sup>†</sup> Permanent address: Institute of Physics, Polish Academy of Sciences, Al. Lotników 32–46, PL-02668 Warsaw, Poland.

- (1) Olah, G. A. *Acc. Chem. Res.* **1971**, *4*, 240–248.
- (2) Waite, J. H.; Young, D. T.; Cravens, T. E.; Coates, A. J.; Crary, F. J.; Magee, B.; Westlake, J. *Science* **2007**, *316*, 870–875.
- (3) Snow, T. P.; Le Page, V.; Keheyan, Y.; Bierbaum, V. M. *Nature* **1998**, *391*, 259–260.
- (4) Herbst, E.; Le Page, V. *Astron. Astrophys.* **1999**, *344*, 310–316.
- (5) Solca, N.; Dopfer, O. *Angew. Chem., Int. Ed.* **2002**, *41*, 3628–3631.
- (6) Doublerly, G. E.; Ricks, A. M.; Schleyer, P. V. R.; Duncan, M. A. J. *Phys. Chem. A* **2008**, *112*, 4869–4874.
- (7) Jones, W.; Boissel, P.; Chiavarino, B.; Crestoni, M. E.; Fornarini, S.; Lemaire, J.; Maitre, P. *Angew. Chem., Int. Ed.* **2003**, *42*, 2057–2059.

(8) Perkampus, H.-H.; Baumgarten, E. *Angew. Chem., Int. Ed.* **1964**, *3*, 776–783.

(9) Freiser, B. S.; Beauchamp, J. L. *J. Am. Chem. Soc.* **1976**, *98*, 3136–3139.

(10) Rode, M. F.; Sobolewski, A. L.; Dedonder, C.; Jouvet, C.; Dopfer, O. *J. Phys. Chem. A* **2009**, *113*, 5865–5873.

(11) Bouchoux, G.; Yanez, M.; Mo, O. *Int. J. Mass Spectrom.* **1999**, *187*, 241–251.

(12) Zyubina, T. S.; Mebel, A. M.; Hayashi, M.; Lin, S. H. *Phys. Chem. Chem. Phys.* **2008**, *10*, 2321–2331.

(13) Franklin, J. L.; Carroll, S. R. *J. Am. Chem. Soc.* **1969**, *91*, 6564–6569.

(14) Lias, S. G.; Ausloos, P. J. *Chem. Phys.* **1985**, *82*, 3613–3624.

(15) Bowers, M. T.; Elleman, D. D.; Omalley, R. M.; Jennings, K. R. *J. Phys. Chem.* **1970**, *74*, 2583–2589.

others. Also, isomerization of protonated benzene into protonated fulvene was suggested to take place in photodissociation studies.<sup>17</sup>

There are no spectroscopic data on other isomers of  $C_6H_7^+$ . In this contribution we investigated electronic transitions of  $C_6H_7^+$  trapped in neon matrices. Besides protonated benzene, the  $\tilde{A}^1A' \leftarrow \tilde{X}^1A'$  transition of  $\alpha$ -protonated fulvene was observed for the first time. Several isomers of neutral  $C_6H_7$ , produced by neutralization of  $C_6H_7^+$ , are characterized by spectroscopic means. We also observed photoinduced isomerization of cyclic  $C_6H_7$  to an open-chain species and  $\alpha$ -hydrogenated fulvene radical.

## 2. Experimental Section

The setup used previously<sup>19</sup> has been modified.<sup>20</sup> The cations of interest were produced in a hot cathode discharge source from appropriate precursors mixed with helium. Sample was introduced into the central region of the source, close to a tungsten filament heated above 2000 °C. Electrons, emitted from the filament and accelerated to  $\sim 50$  eV to the cylindrical anode, ionized and fragmented the sample.

After extraction from the source, ions were guided using a series of electrostatic lenses through a static bender, where they were separated from neutral molecules, and later to a quadrupole mass filter. Typical  $C_6H_7^+$  ion current on the matrix substrate was 10–30 nA when unity mass resolution was chosen. The mass-selected cations were co-deposited with a mixture of neon and an electron scavenger onto a rhodium-coated sapphire plate kept at 6 K.

Chloromethane diluted with neon in the ratio 1:20 000 was used as an electron scavenger; it suppresses ion neutralization during growth of the matrix. Deposited cations charge the matrix, and the ones arriving subsequently hit a metal surface of the vacuum chamber and release electrons. The latter are attracted to the matrix and captured by chloromethane molecules, which are unstable in the anionic form and dissociate into  $CH_3$  and  $Cl^-$ .<sup>21</sup> The  $Cl^-$  anions reduce the space charge of the matrix. The species formed from  $CH_3Cl$ , due to their very low concentration, neither react with the trapped ions nor interfere with measurements of the electronic absorption spectra, because they do not absorb in the 200–1100 nm range.

The detection system used consists of a light source, a spectrograph equipped with three rotatable gratings covering 200–1100 nm, and an open-electrode CCD camera. Absorption spectra were recorded by passing broadband light from halogen or high-pressure xenon lamps through the matrix in a “wave-guide” manner.<sup>22</sup> Light exiting the matrix was collected by a bundle of 50 optical fibers and transferred to the entrance slit of the spectrograph. To eliminate possible photoconversion of the trapped species by the intense, broadband light from the detection system, cutoff filters were used during recording of the spectra. Furthermore, the scans were started from the longest wavelength and continued into the UV. The procedure was later repeated to test whether the species were light sensitive. After these measurements, the matrix was irradiated with a medium-pressure mercury (mpHg) lamp for 30–60 min to neutralize the trapped cations, and the spectra were recorded anew.

$C_6H_7^+$  cations were produced in the source from a number of precursors: 1,3- and 1,4-cyclohexadiene (1,3-CHD and 1,4-CHD), allene, propyne, 1,3,5-hexatriene, and methylcyclopentadiene dimer

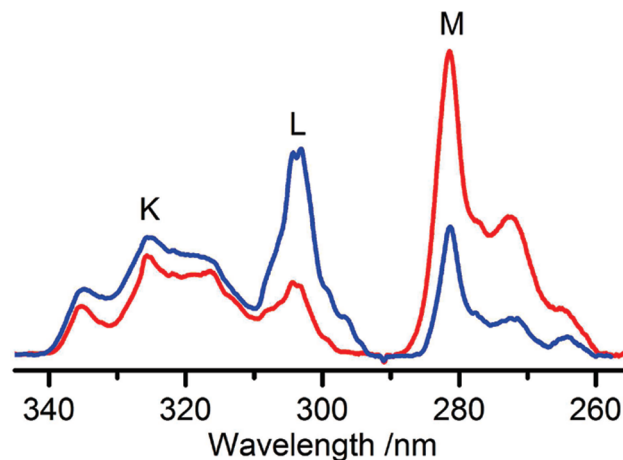


**Figure 1.** UV part of the absorption spectrum recorded after deposition of  $C_6H_7^+$  cations produced from 1,3-cyclohexadiene in a neon matrix with  $CH_3Cl$  scavenger (blue line) and after photobleaching with UV photons (red). K represents absorption of  $C_6H_7^+$  isomers; L and M belong to different isomers of neutral  $C_6H_7$ .

(MCPD). All samples were outgassed by freeze–pump–thaw cycles before use and later mixed with He in the ratio 1:4 for CHD and 1:1 for allene or propyne as precursor. Additionally, reaction of  $H_3^+$  with benzene trapped in a neon matrix has been investigated.  $H_3^+$  was produced from  $H_2$  in the hot cathode ion source and was co-deposited with a benzene/Ne mixture onto the matrix substrate. The ratio of  $C_6H_6/Ne$  was 1:9000, and the deposited charge of  $H_3^+$  was around 1 mC.

## 3. Observations

**3.1.  $C_6H_7^+$  Cations.** The UV part of the absorption spectrum recorded after deposition of mass-selected  $C_6H_7^+$  species produced from a mixture of 1,3-CHD/He is presented in Figure 1 (blue line). It is characterized by three distinct absorption systems (K, L, and M). The K system is a broad, structured absorption with onset at 335 nm. Band systems L and M, with onsets at 310 and 282 nm, are much narrower. The K and L absorptions decrease, though to a different extent, upon UV irradiation of the matrix with a mpHg lamp equipped with water and a  $\lambda \geq 293$  nm cutoff filters. System M gains intensity under these conditions, which is indicative of its neutral origin (Figure 1, red line).

Absorptions K and L could originate from  $C_6H_7^+$  cations or from photo-unstable  $C_6H_7$  neutrals, which could convert to other isomers. UV irradiation of the matrix causes neutralization of the trapped cations by electrons released from the  $Cl^-$  counterions. This process is operative only if the photon energy exceeds the detachment threshold of  $Cl^-$ . The electron affinity of Cl is 3.61 eV in the gas phase,<sup>23</sup> which corresponds to photon wavelengths  $\lambda < 343$  nm. However, the detachment threshold of  $Cl^-$  in a neon matrix is higher than that in the gas phase, due to the surrounding neon atoms, and requires photons with  $\lambda < 300$  nm. Consequently, cations were neutralized using a  $\lambda \geq 293$  nm cutoff filter. A more pronounced effect was observed when full UV radiation of the mpHg lamp was used.

In order to ascertain whether K and L come from  $C_6H_7^+$  or from photo-unstable  $C_6H_7$  neutrals, the cations were also deposited without an electron scavenger. In such experiments, free electrons neutralize cations during growth of the matrix. The UV section of the spectrum obtained is shown in Figure 2

(16) Bouchoux, G.; Nguyen, M. T.; Salpin, J. Y. *J. Phys. Chem. A* **2000**, *104*, 5778–5786.

(17) Zhu, Z. Q.; Gaumann, T. *Org. Mass Spectrom.* **1993**, *28*, 1111–1118.

(18) Herman, J. A.; Herman, K.; McMahon, T. B. *Can. J. Chem.* **1991**, *69*, 2038–2043.

(19) Freivogel, P.; Fulara, J.; Lessen, D.; Forney, D.; Maier, J. P. *Chem. Phys.* **1994**, *189*, 335–341.

(20) Fulara, J.; Nagy, A.; Garkusha, I.; Maier, J. P. *J. Chem. Phys.* **2010**, *133*, 024304.

(21) Zhou, Z. Y.; Xing, Y. M.; Gao, H. W. *J. Mol. Struct.: THEOCHEM* **2001**, *542*, 79–87.

(22) Rossetti, R.; Brus, L. E. *Rev. Sci. Instrum.* **1980**, *51*, 467–470.

(23) Martin, J. D. D.; Hepburn, J. W. *J. Chem. Phys.* **1998**, *109*, 8139–8142.

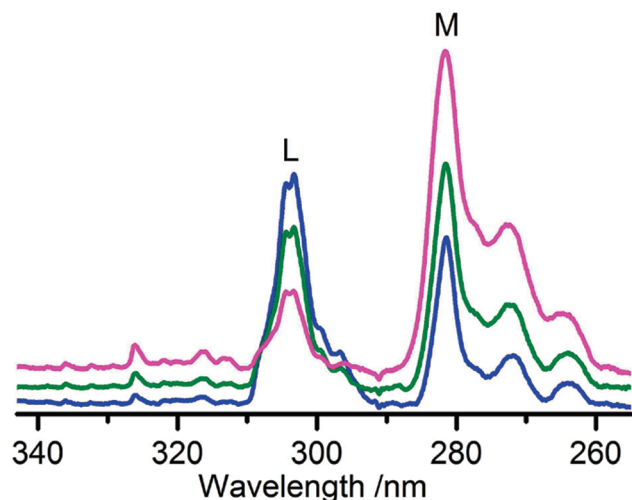


**Figure 2.** UV part of the absorption spectrum recorded after deposition of  $\text{C}_6\text{H}_7^+$  cations produced from 1,4-cyclohexadiene in a pure neon matrix (blue line), after 5 (green) and 20 min (magenta) irradiation with a high-pressure Xe lamp using a  $\lambda \geq 305$  nm cutoff filter. Isomer L of  $\text{C}_6\text{H}_7$  converts to isomer M upon photobleaching with UV photons.

(blue trace). The K system is absent, while L and M are still present. Therefore, absorption K originates from  $\text{C}_6\text{H}_7^+$  cations, and L belongs to a photosensitive  $\text{C}_6\text{H}_7$  neutral.

In order to prove the structure of the cation responsible for the K system, several precursors were used for the production and deposition of the  $m/z = 79$  ions: 1,4-CHD, allene, propyne, 1,3,5-hexatriene, and MCPD. In all cases, the K system was present together with the L and M absorptions of neutrals. However, the relative intensities of the bands constituting the K system change slightly, depending on the precursor used. To illustrate this better, the spectra were normalized to the same intensity of the first band of K (Figure 3). This allows two absorption systems originating from two isomers of  $\text{C}_6\text{H}_7^+$  to be distinguished. Their onsets are labeled  $\text{K}_1$  and  $\text{K}_2$ , with wavelengths given in Table 1. The  $\text{C}_6\text{H}_7^+$  isomer, which is responsible for the  $\text{K}_2$  system, is more efficiently produced from 1,3- and 1,4-CHD, while the  $\text{K}_1$  system is more pronounced in the experiments where allene, propyne, and MCPD were used.

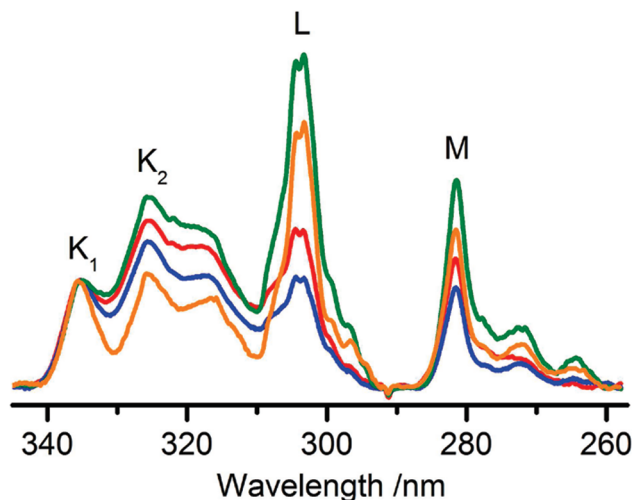


**Figure 3.** Comparison of absorption spectra recorded following deposition of  $\text{C}_6\text{H}_7^+$  cations produced from different precursors. Green line, 1,3-cyclohexadiene; red, 1,4-cyclohexadiene; blue, allene; orange, methylcyclopentadiene dimer.  $\text{K}_1$  is assigned to  $\alpha$ -protonated fulvene,  $\text{K}_2$  to protonated benzene, L to  $c\text{-C}_6\text{H}_7$ , and M to (*E*)-1,4,5-hexatrien-3-yl radical.

**Table 1.** Observed Onsets and Vibrational Progressions within Electronic Transitions of  $\text{C}_6\text{H}_7^+$  and their Neutrals in 6 K Neon Matrices

| species                           | $\lambda/\text{nm}$ | $\bar{\nu}/\text{cm}^{-1}$ | $\Delta\bar{\nu}/\text{cm}^{-1}$ | assignment                         |  |
|-----------------------------------|---------------------|----------------------------|----------------------------------|------------------------------------|--|
| $\alpha\text{-PF}^+$              | 335.3               | 29 822                     | 0                                | $0_0^0$                            | $\tilde{\text{A}} \ ^1\text{A}' \leftarrow \tilde{\text{X}} \ ^1\text{A}'$   |
| $\text{PB}^+$                     | 325.4               | 30 727                     | 0                                | $0_0^0$                            | $\tilde{\text{A}} \ ^1\text{B}_2 \leftarrow \tilde{\text{X}} \ ^1\text{A}_1$ |
|                                   | 316.3               | 31 619                     | 892                              | $\nu_{11}$                         |  |
| $\alpha\text{-HF}$                | 532.4               | 18 782                     | 0                                | $0_0^0$                            |  |
|                                   | 511.2               | 19 560                     | 778                              | $\nu_{20}$                         |  |
|                                   | 326.1               | 30 661                     | 0                                | $0_0^0$                            |  |
|                                   | 319.7               | 31 283                     | 622                              | $\nu_{21}$ (or $5\nu_{14}$ of MHF) |  |
|                                   | 316.6               | 31 584                     | 923                              | $\nu_{17}$                         |  |
|                                   | 313.6               | 31 886                     | 1225                             | $\nu_{13}$                         |  |
| MHF                               | 312.3               | 32 017                     | 1356                             | $\nu_{11}$                         |  |
|                                   | 335.7               | 29 789                     | 0                                | $0_0^0$                            |  |
|                                   | 332.1               | 30 111                     | 322                              | $\nu_{14}$                         |  |
|                                   | 328.9               | 30 403                     | 614                              | $2\nu_{14}$                        |  |
| <i>E</i> -HT                      | 322.0               | 31 055                     | 1266                             | $4\nu_{14}$                        |  |
|                                   | 281.5               | 35 524                     | 0                                | $0_0^0$                            |  |
|                                   | 272.3               | 36 718                     | 1194                             | $\nu_{19}$                         |  |
|                                   | 263.6               | 37 930                     | 2406                             | $2\nu_{19}$                        |  |
| <i>c</i> - $\text{C}_6\text{H}_7$ | 548.9               | 18 217                     | 0                                | $0_0^0$                            | $\tilde{\text{A}} \ ^2\text{A}_2 \leftarrow \tilde{\text{X}} \ ^2\text{B}_1$ |
|                                   | 537.6               | 18 602                     | 385                              | $2\nu_{23}$                        |  |
|                                   | 524.8               | 19 056                     | 839                              | $\nu_{11}$                         |  |
|                                   | 520.5               | 19 212                     | 995                              | $\nu_{10}$                         |  |
|                                   | 516.7               | 19 353                     | 1138                             | $\nu_8$                            |  |
|                                   | 507.3               | 19 714                     | 1497                             | $\nu_5$                            |  |
|                                   | 310.3               | 32 225                     | 0                                | $0_0^0$                            |  |
|                                   | 308.4               | 32 430                     | 205                              | $2\nu_{23}$                        |  |
| <i>B</i>                          | 306.4               | 32 642                     | 417                              | $4\nu_{23}$                        | $\tilde{\text{B}} \ ^2\text{B}_1 \leftarrow \tilde{\text{X}} \ ^2\text{B}_1$ |
|                                   | 304.5               | 32 843                     | 618                              | $6\nu_{23}$                        |  |
|                                   | 302.8               | 33 021                     | 796                              | $\nu_{11}$                         |  |
|                                   | 301.0               | 33 222                     | 997                              | $\nu_{11} + 2\nu_{23}$             |  |
|                                   | 299.2               | 33 427                     | 1202                             | $\nu_{11} + 4\nu_{23}$             |  |
|                                   | 297.2               | 33 647                     | 1422                             | $\nu_{11} + 6\nu_{23}$             |  |
|                                   |                     |                            |                                  |                                    |  |
|                                   |                     |                            |                                  |                                    |  |

**3.2.  $\text{C}_6\text{H}_7$  Neutrals.** As explained above, absorptions L and M (Figure 1) originate from two isomers of  $\text{C}_6\text{H}_7$ . Besides these, several weaker bands are seen on the long-wavelength side of system L. Absorption L decays in a regular way after 5 and 15 min irradiation of the matrix with a high-pressure Xe lamp equipped with a  $\lambda \geq 305$  nm cutoff filter (Figure 2). Parallel to this, M and the weak band system in the range 310–340 nm increase. This indicates that isomer L of  $\text{C}_6\text{H}_7$  photoconverts to isomer M and to another neutral, which is responsible for the weak band system.

Deposition of  $\text{C}_6\text{H}_7^+$  produced from 1,4-CHD into a pure neon matrix resulted not only in the appearance of the UV absorptions seen in Figure 2, but also in the weak 510–550 nm system D. In order to show the relative intensities of the observed features, the visible and UV sections of the spectrum were scaled by appropriate factors in Figure 4 (trace a). The spectrum measured after UV irradiation of the matrix is depicted in trace a'. Band D, with onset at 549 nm, decays after UV irradiation in a similar manner as absorption L, and simultaneously, a weak band at 532 nm grows in intensity.

All the absorptions shown in Figure 4, trace a, were also observed in the spectrum recorded following deposition of  $\text{H}_3^+$  ions into a matrix containing benzene and neon in the ratio 1:9000. The resulting absorption is trace b of Figure 4, and trace b' after UV irradiation. Traces a and b are similar; even the multiplet structure of the origin band at 549 nm is well



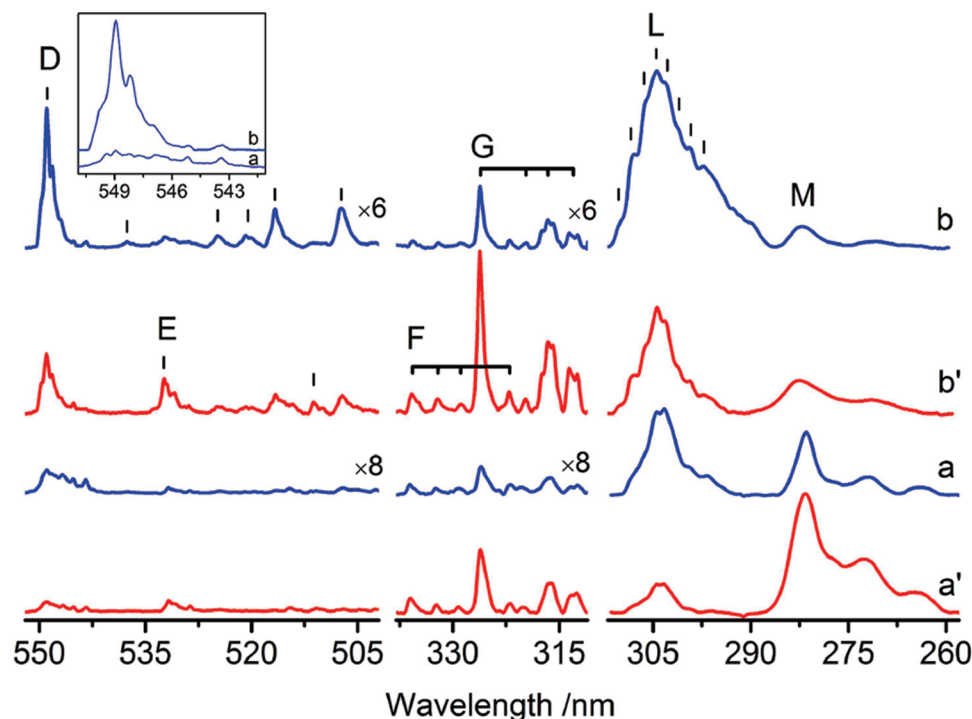


**Figure 4.** Absorption spectra recorded after deposition of  $C_6H_7^+$  into a neon matrix without an electron scavenger. Trace a, after deposition of  $C_6H_7^+$  from 1,4-cyclohexadiene; b, after co-deposition of  $H_3^+$  ions with benzene/Ne = 1:9000; a' and b', recorded after photobleaching with  $\lambda \geq 293$  nm. Bands D and L are assigned to  $c\text{-}C_6H_7$ , E and G to  $\alpha$ -hydrogenated fulvene, F to methyl-hydrogenated fulvene, and M to (*E*)-1,4,5-hexatrien-3-yl radical. Spectra a and a' in the 340–310 nm range as well as in the 550–505 nm range are normalized by a factor of 8; spectra b and b' are normalized by a factor of 6.

reproduced (inset of Figure 4). All the band systems except M are much stronger than in the experiment carried out with mass-selected  $C_6H_7^+$ . No electron scavenger was used in the experiment with  $H_3^+$  ions, and the deposited charge was several times larger than in the case of  $C_6H_7^+$ . Under such conditions, only neutral molecules should be present in the matrix, because without an electron scavenger,  $H_3^+$  should be completely neutralized. The dissociative electron recombination of  $H_3^+$  leads to formation of H and  $H_2$ . Hydrogen atoms are mobile and reactive, even in solid neon at 6 K. One could expect that the main reaction product of H with benzene is the cyclohexadienyl radical,  $c\text{-}C_6H_7$ . Addition of the first hydrogen atom to benzene has an energy barrier around 16 kJ/mol;<sup>24,25</sup> it can be overcome due to the ability of hydrogen to tunnel through the reaction entrance barrier. Electronic transitions of  $c\text{-}C_6H_7$  have been reported.<sup>26–29</sup> According to these, absorption systems L and D, with origins at 549 and 310 nm, can be assigned to the  $\tilde{A}^2A_2 \leftarrow \tilde{X}^2B_1$  and  $\tilde{B}^2B_1 \leftarrow \tilde{X}^2B_1$  electronic transitions of  $c\text{-}C_6H_7$  ( $C_{2v}$  symmetry).

#### 4. Computational Results

A number of structural isomers of  $C_6H_7^+$  are possible. Theoretical calculations predict that the most stable is protonated benzene ( $PB^+$ ), and higher in energy are protonated fulvenes ( $PF^+$ ) and open-chain structures.<sup>11,12</sup> We considered six lowest

energy isomers of  $C_6H_7^+$ :  $PB^+$ ,  $\alpha$ - and  $\beta$ -protonated fulvene ( $\alpha\text{-}PF^+$  and  $\beta\text{-}PF^+$ ), methyl-protonated fulvene ( $MPF^+$ ), and two open-chain forms, (*Z*)- and (*E*)-1,4,5-hexatrien-3-ylum ( $Z\text{-}HT^+$  and  $E\text{-}HT^+$ ) (Figure 5). Geometries of the  $C_6H_7^+$  cations were optimized with DFT at the B3LYP/cc-pVTZ level of theory using the Gaussian 03 program suite.<sup>30</sup> In all cases, real minima were found. All the considered  $C_6H_7^+$  cations except  $MPF^+$  have singlet ground state. For the latter, calculations predict triplet ground state, similar to the cyclopentadienyl cation ( $C_5H_5^+$ ),<sup>31</sup> locating it 3.1 kJ/mol lower than the singlet state. The global minimum on the potential energy surface of  $C_6H_7^+$  is the  $\tilde{X}^1A_1$  state of  $PB^+$ . The next lowest energy isomer,  $\alpha\text{-}PF^+$ , lies 39.3 kJ/mol higher.  $\beta\text{-}PF^+$  was found 108.4 kJ/mol above  $PB^+$ . These data can be compared with the energies 40 and 103 kJ/mol calculated for  $\alpha$ - and  $\beta\text{-}PF^+$  at a higher level of theory, G2(MP2).<sup>11</sup> The other three ions,  $MPF^+$ ,  $E\text{-}HT^+$ , and  $Z\text{-}HT^+$ , are located  $\sim 134$ , 137, and 147 kJ/mol above  $PB^+$ .

The  $C_6H_7$  radicals, which can be obtained by neutralization of the above-discussed cations, have also been studied with DFT at the B3LYP/cc-pVTZ level of theory. Again, the lowest energy isomer is the neutral  $c\text{-}C_6H_7$  derived from protonated benzene. The relative energies of the other isomers of  $C_6H_7$  in their doublet ground state with respect to the  $\tilde{X}^2B_1$  state of  $c\text{-}C_6H_7$  are indicated in Figure 5.

More relevant to the present spectroscopic studies are the electronic excitation energies of the cations and neutrals of  $C_6H_7$  from their ground state. These were calculated between the singlet manifolds of the  $C_6H_7^+$  cations using a time-dependent (TD) DFT method, and the geometries of the ions were optimized using the B3LYP functional and the cc-pVTZ basis

(24) Knutti, R.; Bühler, R. E. *Chem. Phys.* **1975**, 7, 229–243.

(25) Nicovich, J. M.; Ravishankara, A. R. *J. Phys. Chem.* **1984**, 88, 2534–2541.

(26) Shida, T.; Hanazaki, I. *Bull. Chem. Soc. Jpn.* **1970**, 43, 646–651.

(27) Krauss, M.; Osman, R. *Chem. Phys. Lett.* **1995**, 239, 258–262.

(28) Imamura, T.; Zhang, W. J.; Horiuchi, H.; Hiratsuka, H.; Kudo, T.; Obi, K. *J. Chem. Phys.* **2004**, 121, 6861–6867.

(29) Nakajima, M.; Schmidt, T. W.; Sumiyoshi, Y.; Endo, Y. *Chem. Phys. Lett.* **2007**, 449, 57–62.

(30) Frisch, M. J.; et al. *Gaussian 03*, Revision C.01; Gaussian, Inc.: Wallingford, CT, 2004.

(31) Wörner, H. J.; Merkt, F. *Angew. Chem., Int. Ed.* **2006**, 45, 293–296.

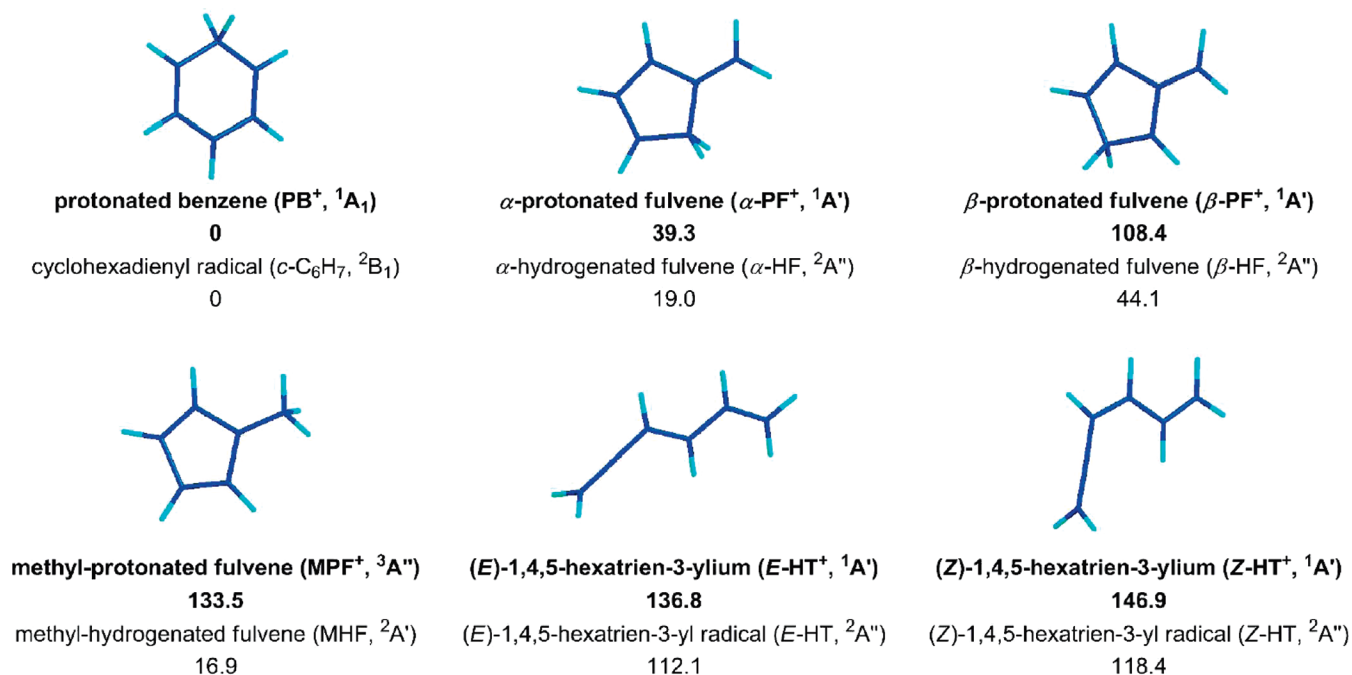


**Figure 5.** Schematic representation of the  $\text{C}_6\text{H}_7^+$  cations (**bold**) and their neutral counterparts (normal font). Relative energies with respect to the most stable isomer are given in kJ/mol. Ground-state geometries were optimized with DFT at the B3LYP/cc-pVTZ level of theory.

set. The calculations predict for  $\text{PB}^+$  two allowed electronic transitions at 4.17 and 5.41 eV with oscillator strengths 0.11 and 0.004. These results agree well with more advanced *ab initio* methods (4.09 and 5.71 eV,  $f = 0.14$  and 0.096).<sup>10</sup> The TD DFT excitation energies for the considered isomers of  $\text{C}_6\text{H}_7^+$  are collected in Table 2. One can expect that these transition energies are predicted with comparable accuracy as for  $\text{PB}^+$ . A striking difference between the calculated oscillator strengths of the UV transition of different isomers of  $\text{PF}^+$  is apparent in Table 2. These indicate a strong transition at 4.35 eV for  $\alpha\text{-PF}^+$  and a weak one in this region for  $\beta\text{-PF}^+$  and  $\text{MPF}^+$ .

The excitation energies of the  $\text{C}_6\text{H}_7^+$  isomers were also calculated using the complete active space self-consistent field method (CASSCF) and the 6-311G(d,p) basis set. The active space consisted of four valence electrons distributed on six orbitals (CAS(4,6)). CASSCF calculations for  $\text{C}_6\text{H}_7^+$  cations were carried out in order to compare the excitation energies with those from TD DFT. The CASSCF method provides a crude approximation to the excited-state energy, as it takes into account only a static electron correlation effect. The general excitation pattern obtained by the CASSCF and TD DFT methods is similar; however, energies predicted by the former are higher than those from the latter.

Similar calculations were carried out for  $\text{C}_6\text{H}_7$  neutrals. Five  $\pi$  valence electrons distributed on six orbitals formed the active space (CAS(5,6)). The CAS(5,6)/6-311G(d,p) calculations predict for  $c\text{-C}_6\text{H}_7$  two dipole-allowed electronic transitions at 2.69 and 4.27 eV, which can be compared with 2.26 and 4.0 eV from the experimental data. The excitation energies for all the considered  $\text{C}_6\text{H}_7$  isomers are collected in Table 2.

## 5. Discussion

**5.1.  $\text{C}_6\text{H}_7^+$  Cations.**  $\text{PB}^+$  is the most stable form of  $\text{C}_6\text{H}_7^+$ , and the absorptions of  $c\text{-C}_6\text{H}_7$  resulted from the neutralization of  $\text{PB}^+$  in a neon matrix. Therefore, one can expect that one of the systems,  $\text{K}_1$  or  $\text{K}_2$ , seen in Figures 1 and 3 originates from the  $\text{PB}^+$  cation. The onsets of these transitions in a neon matrix

lie at 3.7 and 3.81 eV, respectively, which are close to the 4.17 eV excitation calculated by the TD DFT method and the more advanced *ab initio* level of theory (4.09 eV).<sup>10</sup> Both methods predict a strong transition of  $\text{PB}^+$  in the UV region, with the oscillator strength of 0.11 (TD DFT) and 0.14 (*ab initio*). Therefore, one of these absorptions ( $\text{K}_1$  or  $\text{K}_2$ ) must originate from  $\text{PB}^+$ .

Gas-phase kinetic studies on  $\text{C}_6\text{H}_7^+$  produced from different precursors have revealed at least two isomers, which differ in reactivity toward conjugate bases; the more reactive is  $\text{PB}^+$ . The highest relative abundance of non-benzenium ions was observed when  $\text{C}_6\text{H}_7^+$  ions were generated from 1,4-CHD, and the abundance decreased in the precursor series allene > propyne > 1,3-CHD.<sup>14</sup> The mechanism of  $\text{C}_6\text{H}_7^+$  production from various precursors is likely to be different. In the case of CHDs,  $\text{C}_6\text{H}_7^+$  is formed by removing one hydrogen atom. The aromatic ring should stay intact, and the resultant cation should possess the benzenium ion structure. One could expect formation of some noncyclic cation from allene or propyne in a following reaction:



because  $\text{C}_3\text{H}_3^+$  dominates the mass spectrum. MCPD should give rise to ions containing a five-membered ring.

The structure of ions is not always foretold by the geometry of the precursor used. The relative population of  $\text{C}_6\text{H}_7^+$  isomers depends on the kinetics of ion–molecule reactions in the ion source as well as on the energetics of ions. The ions in the source have enough excess energy to overcome barriers and may isomerize to structures different from the precursor used.

Figure 3 shows that the relative intensities of band systems  $\text{K}_1$  and  $\text{K}_2$  change with the precursor used. The strongest relative absorption of the  $\text{K}_2$  system was observed when 1,3-CHD was used. The highest population of the  $\text{PB}^+$  cations has been observed in the kinetic gas-phase studies carried out with this precursor.<sup>14</sup> Therefore, we assign the  $\text{K}_2$  system to the  $\tilde{\text{A}} \ ^1\text{B}_2 \leftarrow \tilde{\text{X}} \ ^1\text{A}_1$  transition of this cation. The position of this

**Table 2.** Excitation Energies of the Most Stable Isomers of  $C_6H_7^+$  and their Neutrals<sup>a</sup>

| species                                 | $S_1/D_1$                   |               |                   |       | $S_2/D_2$                   |               |                   |       | $S_3/D_3$                   |               |              |       |
|---|-----------------------------|---------------|-------------------|-------|-----------------------------|---------------|-------------------|-------|-----------------------------|---------------|--------------|-------|
|   | sym                         | $\Delta E/eV$ | $\lambda/nm$      | $f$   | sym                         | $\Delta E/eV$ | $\lambda/nm$      | $f$   | sym                         | $\Delta E/eV$ | $\lambda/nm$ | $f$   |
| PB <sup>+</sup>                         | <sup>1</sup> B <sub>2</sub> | 4.17          | 298               | 0.11  | <sup>1</sup> A <sub>2</sub> | 5.05          | 245               | 0     | <sup>1</sup> B <sub>1</sub> | 5.41          | 229          | 0.004 |
| <sup>1</sup> A <sub>1</sub>             |                             | <b>4.36</b>   | <b>284</b><br>325 |       |                             | <b>5.33</b>   | <b>233</b>        |       |                             | <b>8.10</b>   | <b>153</b>   |       |
| $\alpha$ -PF <sup>+</sup>               | <sup>1</sup> A'             | 4.35          | 285               | 0.29  | <sup>1</sup> A''            | 4.96          | 250               | 0     | <sup>1</sup> A'             | 5.21          | 238          | 0.056 |
| <sup>1</sup> A'                         |                             | <b>4.58</b>   | <b>271</b><br>335 |       |                             | <b>5.04</b>   | <b>246</b>        |       |                             | <b>7.97</b>   | <b>156</b>   |       |
| $\beta$ -PF <sup>+</sup>                | <sup>1</sup> A'             | 2.06          | 603               | 0.009 | <sup>1</sup> A''            | 4.58          | 271               | 0     | <sup>1</sup> A''            | 5.09          | 243          | 0.002 |
| <sup>1</sup> A'                         |                             | <b>2.47</b>   | <b>502</b>        |       |                             | <b>5.70</b>   | <b>218</b>        |       |                             |               |              |       |
| MPF <sup>+</sup>                        | <sup>3</sup> A''            | 3.45          | 359               | 0.018 | <sup>3</sup> A'             | 3.72          | 333               | 0.048 | <sup>3</sup> A'             | 4.03          | 308          | 0     |
| <sup>3</sup> A''                        |                             | <b>3.58</b>   | <b>346</b>        |       |                             | <b>3.79</b>   | <b>327</b>        |       |                             | <b>6.53</b>   | <b>190</b>   |       |
| Z-HT <sup>+</sup>                       | <sup>1</sup> A''            | 3.11          | 399               | 0     | <sup>1</sup> A'             | 4.26          | 291               | 0.60  | <sup>1</sup> A''            | 5.36          | 231          | 0     |
| <sup>1</sup> A'                         |                             | <b>4.48</b>   | <b>277</b>        |       |                             | <b>5.44</b>   | <b>228</b>        |       |                             | <b>8.22</b>   | <b>151</b>   |       |
| E-HT <sup>+</sup>                       | <sup>1</sup> A''            | 3.14          | 395               | 0     | <sup>1</sup> A'             | 4.43          | 280               | 0.86  | <sup>1</sup> A''            | 5.40          | 229          | 0     |
| <sup>1</sup> A'                         |                             | <b>4.74</b>   | <b>262</b>        |       |                             | <b>5.48</b>   | <b>226</b>        |       |                             | <b>8.37</b>   | <b>148</b>   |       |
| <i>c</i> -C <sub>6</sub> H <sub>7</sub> |                             | <b>2.69</b>   | <b>461</b><br>549 |       |                             | <b>4.27</b>   | <b>290</b><br>310 |       |                             | <b>6.11</b>   | <b>202</b>   |       |
| <sup>2</sup> B <sub>1</sub>             |                             |               |                   |       |                             |               |                   |       |                             |               |              |       |
| $\alpha$ -HF                            |                             | <b>2.70</b>   | <b>459</b><br>532 |       |                             | <b>4.16</b>   | <b>298</b><br>326 |       |                             | <b>6.56</b>   | <b>189</b>   |       |
| <sup>2</sup> A''                        |                             |               |                   |       |                             |               |                   |       |                             |               |              |       |
| $\beta$ -HF                             |                             | <b>2.88</b>   | <b>431</b>        |       |                             | <b>4.51</b>   | <b>275</b>        |       |                             | <b>6.01</b>   | <b>206</b>   |       |
| <sup>2</sup> A''                        |                             |               |                   |       |                             |               |                   |       |                             |               |              |       |
| MHF                                     |                             | <b>0.96</b>   | <b>1292</b>       |       |                             | <b>4.13</b>   | <b>300</b><br>336 |       |                             | <b>6.66</b>   | <b>186</b>   |       |
| <sup>2</sup> A'                         |                             |               |                   |       |                             |               |                   |       |                             |               |              |       |
| Z-HT                                    |                             | <b>2.76</b>   | <b>449</b>        |       |                             | <b>4.26</b>   | <b>291</b>        |       |                             | <b>6.82</b>   | <b>182</b>   |       |
| <sup>2</sup> A''                        |                             |               |                   |       |                             |               |                   |       |                             |               |              |       |
| E-HT                                    |                             | <b>2.83</b>   | <b>438</b>        |       |                             | <b>4.23</b>   | <b>293</b><br>282 |       |                             |               |              |       |
| <sup>2</sup> A''                        |                             |               |                   |       |                             |               |                   |       |                             |               |              |       |

<sup>a</sup> Excitation energies for cations were calculated with TD DFT at the B3LYP/cc-pVTZ (normal font) and CAS(4,6)/6-311G(d,p) (**bold**) level of theory, and for neutral C<sub>6</sub>H<sub>7</sub> at the CAS(5,6)/6-311G(d,p) level of theory (**bold**); *italics* indicate observed data.

absorption agrees well with the gas-phase photodissociation spectrum<sup>9</sup> of PB<sup>+</sup>. The band lying  $\sim 890\text{ cm}^{-1}$  above the origin can be assigned to the excitation of the  $\nu_{11}$  vibrational mode in the  $\tilde{A}^1B_2$  state. In the earlier PD experiments, a much weaker absorption of PB<sup>+</sup> was detected at  $\sim 245\text{ nm}$ ,<sup>9</sup> and the recent theoretical calculations<sup>10</sup> predict two excited states, <sup>1</sup>A<sub>1</sub> and <sup>1</sup>B<sub>1</sub>, in this region, which are dipole accessible from the ground state. However, the oscillator strengths of these transitions are much weaker (0.096 and 0.005, respectively) than that to the  $\tilde{A}^1B_2$  state. This transition was not observed in these measurements due to low transmittance in this region caused by scattered light.

The K<sub>1</sub> band system can be assigned to  $\alpha$ -PF<sup>+</sup> for the following reasons. The highest intensity ratio of the absorption K<sub>1</sub> to K<sub>2</sub> was observed with the MCPD precursor (Figure 3, bottom trace), in which a five-membered ring could survive the conditions in the ion source. Among the protonated fulvenes,  $\alpha$ -PF<sup>+</sup> is the most stable structure, and TD DFT calculations predict a strong electronic transition only for  $\alpha$ -PF<sup>+</sup> (at 4.35 eV), close to the observed K<sub>1</sub> system (3.7 eV). The oscillator strength of the UV transition of  $\alpha$ -PF<sup>+</sup> is ca. 3 times larger than for PB<sup>+</sup> and is about 2 orders of magnitude higher than for the other protonated fulvenes ( $\beta$ -PF<sup>+</sup> and MPF<sup>+</sup>).

**5.2. Neutral C<sub>6</sub>H<sub>7</sub>.** The deposition of mass-selected C<sub>6</sub>H<sub>7</sub><sup>+</sup> with all the precursors used has resulted in the appearance of the strong 310 nm band system and the weaker one with onset at 549 nm for the neutral cyclohexadienyl radical, *c*-C<sub>6</sub>H<sub>7</sub>. This

radical was observed as a result of partial neutralization of C<sub>6</sub>H<sub>7</sub><sup>+</sup>, even in the experiments when an electron scavenger was added into the matrix. The origin band of *c*-C<sub>6</sub>H<sub>7</sub> at 549 nm is sharp, and a multiplet structure is apparent. Two modes of energy, 27 and 71 cm<sup>-1</sup>, form this pattern. These frequencies are too low to be assigned to any vibration of this molecule; they are due to coupling of the phonons of the neon lattice to the electronic state of *c*-C<sub>6</sub>H<sub>7</sub>. The  $\tilde{A}^2A_2 \leftarrow \tilde{X}^2B_1$  transition of *c*-C<sub>6</sub>H<sub>7</sub> with onset at 549 nm has a well-evolved vibrational structure that is formed by the excitation of several totally symmetric fundamental modes in the upper electronic state. The lowest energy vibrational band observed in the spectrum is located  $\sim 385\text{ cm}^{-1}$  above the origin and is assigned to the double excitation of the  $\nu_{23}$  mode of b<sub>1</sub> symmetry. Wavelengths of the observed absorptions of *c*-C<sub>6</sub>H<sub>7</sub> and their assignments are collected in Table 1.

The absorption L of *c*-C<sub>6</sub>H<sub>7</sub> at  $\sim 310\text{ nm}$  has a multiplet structure too. This pattern is well pronounced in the experiment of H<sub>3</sub><sup>+</sup> with benzene trapped in a neon matrix (traces b and b' in Figure 4). Absorption L is much broader than band D, and two frequencies, 205 and 796 cm<sup>-1</sup>, with their overtones and combinations form the observed profile of the UV system. In the ground state of *c*-C<sub>6</sub>H<sub>7</sub>, our calculations predict the lowest energy mode  $\nu_{23}$  at 175 cm<sup>-1</sup> (b<sub>1</sub> symmetry), which corresponds to the out-of-plane ring deformation with a considerable contribution of the out-of-plane motion of the CH<sub>2</sub> group. The

single excitation of this mode is forbidden for the  ${}^2B_1 \leftarrow \tilde{X} {}^2B_1$  transition; therefore, the energy of  $\sim 205\text{ cm}^{-1}$  must correspond to  $2\nu_{23}$ . The frequency difference of the  $\nu_{23}$  mode in the ground and the  $\tilde{B} {}^2B_1$  states is quite large and reflects a geometry change along this coordinate upon electronic excitation. The profile of the absorption at  $\sim 310\text{ nm}$  is dominated by the long progression of the  $205\text{ cm}^{-1}$  overtone bands and its combination with the  $\sim 796\text{ cm}^{-1}$  mode. The frequency of the latter is close to the calculated, totally symmetric  $\nu_{11}$  ( $871\text{ cm}^{-1}$ ) mode.

UV irradiation of  $c\text{-}C_6H_7$  with a mpHg lamp using a  $\lambda \geq 305\text{ nm}$  cutoff filter leads to a decrease of the visible and UV systems of this species and simultaneously increases the strong absorption at  $\sim 282\text{ nm}$  and weaker ones in the  $310\text{--}340\text{ nm}$  and visible ranges (Figure 3). It is well established that 1,3-CHD<sup>32,33</sup> and its cation,<sup>34</sup> which are structurally similar to  $c\text{-}C_6H_7$ , undergo a photoinduced ring-opening reaction leading to 1,3,5-hexatriene or its cation, respectively. In the case of neutral 1,3-CHD, the ring-opening takes place in a fraction of a picosecond, and the product relaxes to the more stable (*i*Zt-hexatriene) form in several tenths of a picosecond.<sup>32</sup> The open-chain structure, produced from 1,3-CHD or 1,3-CHD<sup>+</sup> by the UV-induced ring-opening reaction, absorbs at shorter wavelength than the parent species.

It is expected that a similar process takes place in the case of UV irradiation of  $c\text{-}C_6H_7$ , and the strong band system with onset at  $282\text{ nm}$  is assigned to the open-chain isomer. CAS(5,6)/6-311G(d,p) calculations predict two electronic transitions for the two neutral, open-chain isomers *E*- and *Z*-HT at  $\sim 2.8$  and  $4.2\text{ eV}$ ; the latter transition lies close to the observed M system ( $4.39\text{ eV}$ ). By analogy to the photoisomerization of 1,3-CHD to *i*Zt-hexatriene, the M system is assigned to *E*-HT. The relative absorption of *E*-HT (at  $\sim 282\text{ nm}$ ) with respect to the  $310\text{ nm}$  system of  $c\text{-}C_6H_7$  varies with the experimental conditions. The weakest M absorption was observed in the experiment of  $H_3^+$  with benzene trapped in the matrix. In this case, *E*-HT was present as a result of the ring-opening process of the excited  $c\text{-}C_6H_7$  produced in the exothermic ( $117\text{ kJ/mol}$ ) reaction of  $C_6H_6$  with H generated by neutralization of  $H_3^+$ . The M absorption of *E*-HT was also observed following deposition of  $C_6H_7^+$  without an electron scavenger. In such experiments, *E*-HT was formed by the neutralization of collisionally produced *E*-HT<sup>+</sup> from  $PB^+$  in a neon matrix.

Though the CAS calculations predict the electronic transition of *E*-HT also in the visible range ( $\sim 438\text{ nm}$ ), near the weak E band system with onset at  $532\text{ nm}$ , which grows in intensity upon UV irradiation of the matrix, the system E cannot be assigned to *E*-HT because its relative intensity with respect to absorption at  $\sim 282\text{ nm}$  varies with the experimental conditions. The intensity of the E system correlates well with the G system, with onset at  $326\text{ nm}$ .

After deposition of  $C_6H_7^+$ , the absorption of  $\alpha\text{-}PF^+$  was detected. Thus, neutral  $\alpha$ -hydrogenated fulvene ( $\alpha\text{-HF}$ ) should also be present in the matrix as a result of neutralization of the corresponding ion. CAS calculations predict two transitions at  $459$  and  $298\text{ nm}$  for this neutral, which are quite close to the

observed absorptions at  $532$  and  $326\text{ nm}$ . Therefore, the E and G systems (Figure 4) are assigned to  $\alpha\text{-HF}$  (Table 1). The absorptions at  $532$  and  $326\text{ nm}$  grow in intensity at the expense of  $c\text{-}C_6H_7$  upon UV irradiation. The absorption of UV photons by  $c\text{-}C_6H_7$  leads not only to the ring-opening reaction but also to the photoisomerization to  $\alpha\text{-HF}$ . The latter process is feasible, as the calculated barrier of  $\sim 219\text{ kJ/mol}$ <sup>11</sup> for the isomerization of  $PB^+$  to  $\alpha\text{-}PF^+$  should be similar to the neutral one, and it can be overcome by the electronic excitation of  $c\text{-}C_6H_7$ . The strongest E and G systems are observed in the reaction of  $H_3^+$  with benzene in a neon matrix. The G band is stronger than M in this case, which means that the isomerization to  $\alpha\text{-HF}$  dominates over the ring-opening reaction.

Apart from the discussed L, M, D, E, and G systems in the  $330\text{--}340\text{ nm}$  range, there is a weak F system present which cannot be attributed to  $c\text{-}C_6H_7$ , *E*-HT, or  $\alpha\text{-HF}$  species, because only one transition is predicted for these species in this range. Therefore, the F system is due to another isomer of  $C_6H_7$ . CAS calculations predict a transition around  $300\text{ nm}$  for methylhydrogenated fulvene (MHF) and slightly lower in energy for  $\beta$ -hydrogenated fulvene ( $275\text{ nm}$ ). The F lies close to the literature value for methylcyclopentadienyl radical ( $336\text{ nm}$ ).<sup>35,36</sup> Also the vibrational pattern of the F system is similar. Therefore, absorption F, with the onset at  $336\text{ nm}$ , is assigned to MHF. The excitation of the  $\nu_{14}$  mode and its overtones is observed and agrees well with data reported earlier.<sup>35,36</sup>

## 6. Conclusions

The presented investigations on  $C_6H_7^+$  trapped in a neon matrix provide a direct spectroscopic characterization of two structural isomers of this cation, which have been postulated in the earlier gas-phase reactivity studies.<sup>13–18</sup> We confirm that one of these isomers is protonated benzene, and its electronic spectrum in a neon matrix agrees well with the one obtained in an earlier photodissociation experiment.<sup>9</sup> The second, less reactive isomer of  $C_6H_7^+$  reported in earlier gas-phase studies<sup>14</sup> is identified as  $\alpha$ -protonated fulvene and is characterized spectroscopically for the first time. The electronic transitions  $\tilde{A} {}^1B_2 \leftarrow \tilde{X} {}^1A_1$  of  $PB^+$  and  $\tilde{A} {}^1A' \leftarrow \tilde{X} {}^1A'$  of  $\alpha\text{-}PF^+$  lie in the UV range, and they overlap. This fact will hinder their future gas-phase spectroscopic observation, as both isomers are produced concomitantly from a number of precursors.

Besides cyclohexadienyl radical, three other isomers of  $C_6H_7$  are identified following UV induced neutralization of  $C_6H_7^+$  and characterized spectroscopically for the first time:  $\alpha\text{-HF}$ , MHF, and *E*-HT. Photoinduced isomerization of  $c\text{-}C_6H_7$  to *E*-HT and  $\alpha\text{-HF}$  was observed.

**Acknowledgment.** This work has been supported by the Swiss National Science Foundation (project no. 200020-124349/1).

**Supporting Information Available:** Cartesian coordinates and energies of the cationic and neutral  $C_6H_7$  isomers shown in Figure 5; complete ref 30. This material is available free of charge via the Internet at <http://pubs.acs.org>.

JA106470X

(32) Kuthirummal, N.; Rudakov, F. M.; Evans, C. L.; Weber, P. M. *J. Chem. Phys.* **2006**, *125*, 133307.

(33) Schonborn, J. B.; Sielk, J.; Hartke, B. *J. Phys. Chem. A* **2010**, *114*, 4036–4044.

(34) Shida, T.; Kato, T.; Nosaka, Y. *J. Phys. Chem.* **1977**, *81*, 1095–1103.

(35) Dimauro, L. F.; Heaven, M.; Miller, T. A. *Chem. Phys. Lett.* **1986**, *124*, 489–492.

(36) Yu, L.; Cullin, D. W.; Williamson, J. M.; Miller, T. A. *J. Chem. Phys.* **1991**, *95*, 804–812.